

Compute-aided Differentiation of Focal Liver Disease in MR Imaging

Xuejun Zhang^a, Masayuki Kanematsu^b, Hiroshi Fujita^c, Takeshi Hara^c,
Hiroshi Kondo^b, Xiangrong Zhou^c, Wenguang Li^a and Hiroaki Hoshi^b

^a Graduate School of Engineering, Gifu University, Japan

^b Department of Radiology, Gifu University School of Medicine, Japan

^c Department of Intelligent Image Information, Graduate School of Medicine,
Gifu University, Japan

Abstract

To aid radiologists for their decision of liver diseases in MR imaging, a method based on artificial neural network (ANN) is proposed. The input units correspond to the homogeneity and the intensities within region of interests selected from four MR images. In order to quantify the degree of liver cirrhosis, liver region is extracted from MR or CT images and divided into left and right parts. The ratio of volume in each part may differentiate a normal liver from cirrhosis. The result shows that our ANN based program may provide radiologists with educational use or referential opinion during their practical diagnostic procedure.

Keywords: MR imaging, focal liver disease, artificial neural network, edge detection

1. Introduction

Hepatocellular carcinoma (HCC) is most common primary malignant liver neoplasms. Further, malignant tumor-mimicking conditions such as dysplasia in cirrhosis, cavernous hemangioma, or liver cyst must be accurately diagnosed and differentiated from malignancy, which may predispose to diagnostic dilemma in daily radiologic practice [1]. Early diagnosis provides the opportunity for hepatectomy, liver transplant, or other interventional treatments that may play a curative or palliative role. Magnetic resonance (MR) imaging is now a popular diagnostic tool that allows physicians to precisely examine the internal structure of human body. With the advantage of good spatial and contrast resolutions, MR imaging contributes to detection and characterization of focal liver lesions in radiologic practices. In MR imaging of the liver, radiologists ordinarily interpret several MR images obtained by different pulse sequences with and without contrast enhancement to reach the diagnosis. However, the imaging findings are falsely interpreted in some patients because of the complexity.

Our purpose is to establish a computer-aided diagnosis (CAD) system for distinguishing the pathologies of focal liver lesions and quantitative analysis of the degree of liver cirrhosis on MR images, that helps radiologists integrate the MR imaging findings with different pulse sequences (T1-weighted, T2-weighted, and gadolinium-enhanced MR images) and raises the diagnostic accuracy even with inexperienced radiologists (residents or general radiologists). In this paper, we also propose a fully automatic method of finding the initial liver contour and calculating the gray-level threshold value to reconfirm the final liver region.

2. Materials and Methods

In our study, we selected four types of MR images that were considered most informative on the diagnosis of focal liver disease. Portal venous phase in MR imaging was used for quantitative analysis of the degree of hepatic cirrhosis.

2.1 Differentiation of 5 categories of focal liver disease

The basic concept of the diagnosis of focal liver lesions with MR imaging is based on the difference in signal intensity between liver lesions and liver parenchyma; internal architecture; and vascularity, that is evaluated with T1-weighted images, T2-weighted images, and gadolinium-enhanced images obtained in the hepatic arterial-phase and equilibrium-phase that occurs approximately 25 seconds and 3 minutes, respectively, after initiating intravenous bolus injection of gadolinium-chelate solution.

(a) Artificial Neural Networks: Artificial neural network (ANN), which has been successfully applied in many fields on medical imaging [2], is a method simulated to the way of what human brain working: solving problem by the knowledge studied. Instead of giving a match equation, it uses samples to train the weights between neurons. Once the network is trained, the knowledge is stored in weights. When the input data are provided to the network, it then recalls the response it learned during training. From a former expert trained network, it should be easy for less experienced doctors to make a correct diagnosis by generalizing new inspections from past experience.

We have developed a software named "LiverANN" [3] based on ANN technology for the diagnosis of focal liver disease. The inputs and outputs of ANN are connected with neurons. The algorithm tries to fit very input samples to the corresponding outputs by adjusting the weights among of the neurons, and the accuracy is improved gradually by iterative time. After establishing the relationship function between the inputs and outputs, we apply the ANN to the doctors' practical routine inspection to test the generation ability of ANN.

(b) Architecture of ANN: As shown in Figure 1, our ANN is a conventional fully connected three-layer feed-forward neural network with 5 input units, 8 hidden units and 5 output units. Similar to the inspecting way used in the radiologist's research, we apply the visual features on MR image to the training of network. The 5 input units are the homogeneity of T2-weighted MR imaging and the intensities of four MR imagings: T1-weighted MR imaging, T2-weighted MR imaging, dynamic arterial phase and dynamic equilibrium phase. The outputs are the 5 categories of hepatic diseases: liver cyst, cavernous hemangioma, dysplasia in cirrhosis, hepatocellular carcinoma and metastasis cases.

(c) Input Selection: Our program provides a pan toolbox that allow radiologist to mark the ROI by dragging the mouse as shown in Figure 2, as well as a function to extract and calculate the liver background for future use. In one hepatic MR case, the region of lesions in the images of T1-weighted, T2-weighted, dynamic arterial phase and dynamic equilibrium phase are picked out respectively, then the program automatically calculated the average brightness as the intensity in the ROI, and standard deviation value corresponds to homogeneity. All elements of the training set must be scaled appropriately, the four intensities and T2 homogeneity are normalized into numerical data between 0 and 1 as the input signals of the ANN.

2.2 Quantitative analysis of the degree of liver cirrhosis

A cirrhosis liver is often enlarged in right part and shrunk in left part. We developed an algorithm for segmentation of liver region from other organs and tissues on portal venous phase image as Figure 3(a). Two edge operators are applied to obtain the initial liver area, from which the mean gray value is calculated as threshold value. The final contour is re-detected by using thresholding technique.

(a) Edge detection by combination of Sobel and LOG filters: When applying the thresholding technique to separating the object from background, it is difficult to: 1) determine a proper threshold value and 2) distinguish the connected organs or tissues which sometimes show relatively high or low intensities to liver region, for example, kidney or stomach. Edge detection may settle these problems. By combining an eight directional 3X3 Sobel and Laplacian-of-Gaussian (LOG) filter [4], we can extract the subtle edges that should be missed by each of the individual method. After edge detection, the inside hepatic tissues are turned into black and only remained a closed contour along liver surface as shown in Figure 3(b).

(b) Selecting the liver region: Aorta is an important reference coordinate for its position always locates on the under-right side of liver near caudate lobe. The program can robustly identify aorta coordinate from all labelled white area on Figure 3(b) by analysing circularity, as well as pixel values on original image. Since the liver is the biggest organ in the MR image selected, we can pick up the liver region by the size of labelling. Liver and background region have biggest area in all the connected white pixels, but the position of these two areas is quite different. Liver candidate could be found out among all the labelled white components by maximum area except for background and by referring to information of location (on left side of MRI and upper-left of aorta). Figure 3(c) illustrates a selected liver structure.

(c) Re-detection by thresholding technique: If the contour is not completely closed, undesired parts will connect to the liver region. The main reason of this occasion is that the edge between liver and tissues is indistinct. However, in many cases the intensity between these two structures is various. Therefore, it is possible to use thresholding technique for component decomposition as in Figure 3(c). Holes inside the initial area are filled in so as to make a mask shown in Figure 3(d), from which we may calculate the mean gray-value G_{avr} from restricted original image within the mask area. Livers on MR image often appear to be brighter on the upper side than lower side. Therefore, we apply two threshold values on the restricted original image to reconfirming the upper and lower side liver, which are G_{avr-10} and G_{avr-30} , respectively. Final liver mask is derived from adding area of upper side, lower side liver and aorta region marked as black in Figure 3(d). Eliminated organs are turned into gray.

(d) Three-dimensional segmentation and visualization: The above algorithm is modified to be able to extract small liver region by using the result from last slice. Three-dimensional MR image is constructed from about 25 slices and the surface image can be displayed from different view points by using volume rendering technique. Figure 4(a) and Figure 4(b) show a normal liver and cirrhosis liver, respectively. Also this method may extend to extract liver region or other organs on CT images as shown in Figure 5(a) and Figure 5(b).

(e) Calculating the degree of cirrhosis: Liver is separated into left and right part by drawing a Couinaud line shown in Figure 4(c), and the volume (V) in each part is calculated slice by slice. The degree of liver cirrhosis is defined as $V_{right}/(V_{right}+V_{left})$.

2.3 Study Apparatus and Population

Three hundreds and twenty MR images in 80 patients with focal liver lesions were obtained with a 1.5-T superconducting magnet (Signa Horizon; GE Medical Systems, Milwaukee, Wis). The focal liver lesions were diagnosed by pathognomonic imaging findings with ultrasonographic, computed tomographic (CT), or MR imaging findings; histopathological evaluation with surgery or biopsy; serological tumor marker test results; or follow-up study. Fifty focal liver lesions including liver cysts (n = 10), cavernous hemangiomas (n = 10), dysplasias in cirrhosis (n = 10), hepatocellular carcinoma (n = 10), and metastases (n = 10) were used to train the ANN. The remaining 30 lesions were used for testing the performance of the ANN. Twenty cases were selected for segmenting liver region and 2 cases including normal and cirrhosis liver with multi-slices both in MR and CT images were used for 3D segmentation and visualization.

3. Results

The initial result showed that the LiverANN classified 5 types of liver lesions with a training accuracy of 100% on the 50 cases in the training set and a testing sensitivity of 93.3% (28/30) for the 30 test cases. Our method is robust to separate the liver from other connected organs with error rate (calculated by XOR operation on masks of golden standard and detected liver region) less than 20.0%. The volume ratio was relatively higher in liver cirrhosis with 24.0% (148089/618374) than in the normal cases with 8.7% (84977/576343), as shown in Figure 4(a) and Figure 4(b) respectively. Results of 3D segmentation and visualization were shown in Figure 4 and Figure 5.

4. Conclusions

Our ANN based program demonstrated its ability to fuse the complex relationships among the individual MR imaging inputs, which may lead it to provide radiologists with educational use or referential opinion during their practical diagnostic procedure.

Acknowledgments

This study was supported in part by the Grant-In-Aid for Cancer Research from the Japanese Ministry of Health, Labour and Welfare, as well as Japanese Ministry of Education, Culture, Sports, Science and Technology. The author (X. Z) would like to thank to the Foundation for C&C Promotion for their financial support on the project.

References

- [1] O. Matsui, M. Kadoya, T. Kameyama, et al., "Adenomatous hyperplastic nodules in the cirrhotic liver: Differentiation from hepatocellular carcinoma with MR imaging," *Radiology*, **173**(1), pp.123-126, 1989
- [2] H. Fujita, T. Katafuchi, T. Uehara, et al., "Application of artificial neural network to computer-aided diagnosis of coronary artery disease in myocardial SPECT bull's-eye images," *J. Nucl. Med.* **33**(2), pp.272-276, 1992.
- [3] X. Zhang, M. Kanematsu, H. Fujita, et al. "Computerized classification of liver disease in MRI using artificial neural network", *Proc. SPIE*, **4322**, pp.1735-1742, 2001.
- [4] D. Marr and E. Hildreth, "Theory of edge detection", *Proc. Royal Society of London*, **B207**, pp. 187-217, 1980.

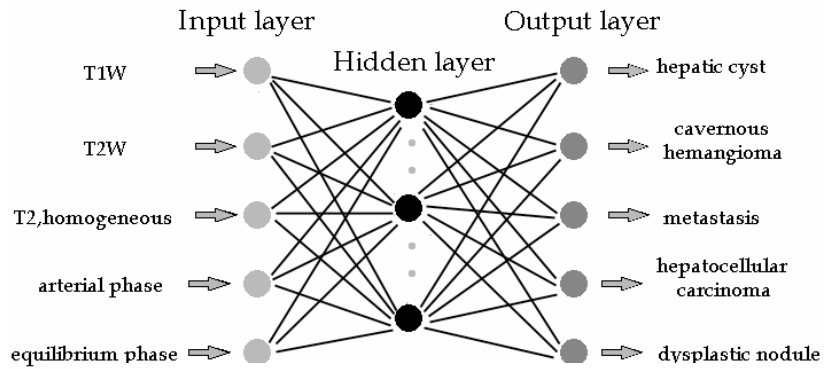


Figure 1: A multi-layer feed forward neural network used in LiverANN

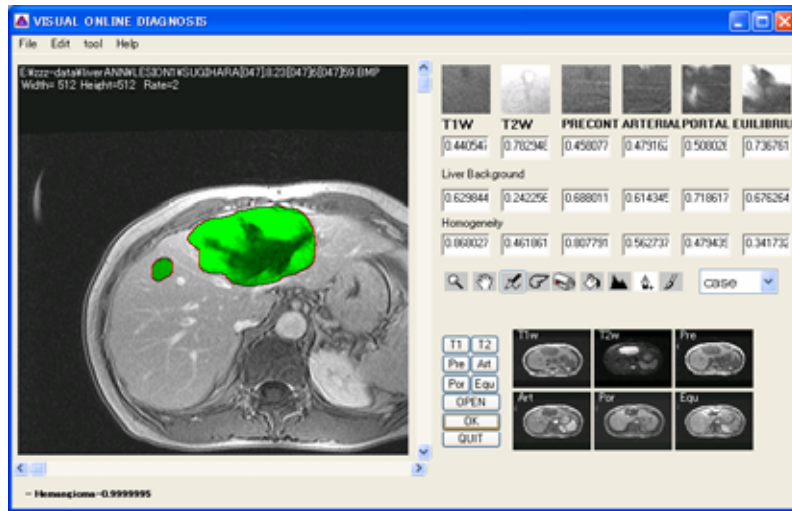


Figure 2: The graphical user interface of the LiverANN developed. The main window is changed when one of the four MR buttons is pressed, corresponding to the T1 and T2 weighted, dynamic arterial and dynamic equilibrium phase images. The four sub-images show the ROIs selected from four MR images by doctor. Intensities and homogeneity of ROI are calculated automatically. Outputs of ANN indicate the possibility (0-1.0) of each liver disease.

LiverANN Doctor	Cyst case	Hemangioma case	Dysplasia case	HCC case	Metastasis case
Cyst	6	0	0	0	0
Hemangioma	0	6	0	0	0
Dysplasia	0	0	6	0	0
HCC	0	0	0	4	2
Metastasis	0	0	0	0	6

Table 1: The classification result of 30 testing cases. Two hepatocellular carcinoma cases judged by a doctor are categorized into metastasis by LiverANN incorrectly.

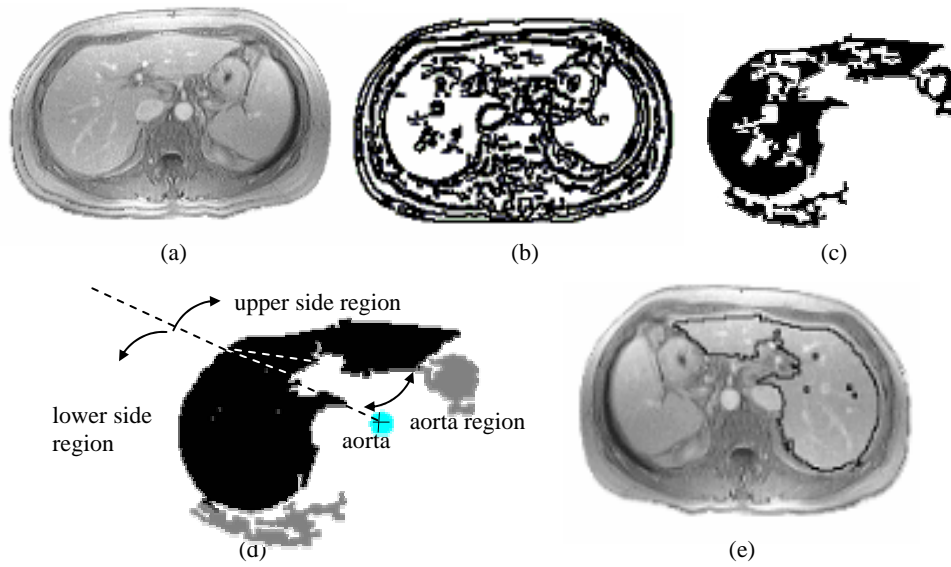


Fig. 3 Procedure of segmentation of liver on MRI. (a) Original image. (b) Binary image after edge detection. (c) Selected initial liver from labeled white area. (d) Re-detection area separated into 3 regions. (e) Reconfirmed liver contour.

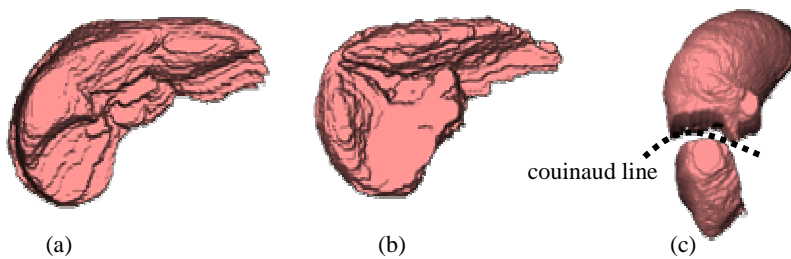


Fig. 4 Livers constructed by extracted 2D liver regions from MR images with a slice interval of 5 mm indicate that the volume ratios between left and right side of liver are different in a normal case (a) and cirrhosis case (b), where a couinaud line is drawn in (c) to separate the two parts.

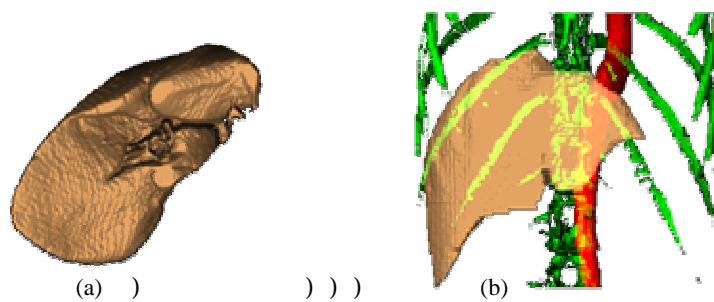


Fig. 5 (a) Livers constructed from CT images with a slice interval of 1.25 mm. (b) Liver, aorta, costa and spine extracted by our same edge detection based method for MR images.